TM_{0n0}- and TM_{m10}-Mode Oversized Cylindrical Cavity Power Combiners

SHIGEJI NOGI AND KIYOSHI FUKUI, MEMBER, IEEE

Abstract—**TM_{m10}-mode power combining is treated in addition to conventional TM_{0n0}-mode combining in a multiple-device oversized cylindrical cavity having a window output structure. Mode analysis gives the condition for stable power-combining operation in the desired mode. By experiments both on TM_{0n0}-mode combining ($n = 2$, 3, and 4) and on TM_{m10}-mode combining ($m = 2$ and 8), it is shown that almost perfect power combining in the TM_{210} mode can be achieved as in the TM_{020} mode and that the power combining efficiency decreases gradually with increasing n or m. A possible advantage of TM_{m10}-mode combining in an oversized cavity is suggested based on the experimental result that power combining in the TM_{810} mode gives higher efficiency than in the TM_{040} mode.**

I. Introduction

IN RECENT YEARS, many power-combining techniques have been developed for high-power solid-state microwave and millimeter-wave sources [1], [2]. Among them, the cylindrical cavity combiners originated by Harp and Stover [3] are the most well known and widely used. Combiners of this type have been developed successfully mainly using TM_{010}- and TM_{020}-mode cavities in the microwave frequency range [4]–[7]. However, several trials for TM_{0n0}-mode ($n \geq 3$) combiners with oversized cavities to accommodate many more active devices have not yet given useful results [1], [8]. It is said that, at higher frequencies, the cylindrical cavity combiners are less practicable because of a more serious moding problem in the oversized cavity, which can accommodate a large number of devices, and because of difficulties in fabricating the output probe of the cavity [2].

The authors recently proposed a window output structure (see Fig. 1) for a cylindrical cavity combiner which facilitates both undesired-mode suppression and fabrication even in the millimeter-wave region, and confirmed that the TM_{020}-mode combiner with this structure had the capability of almost perfect power combining [9], [10]. In [9] it was shown analytically that in addition to the TM_{010} and the TM_{020} mode, the TM_{m10} ($m \geq 1$) modes can also be power-combining modes in this structure. However, the simple equivalent circuit used in [9] cannot support the higher order modes which are in mode competition with the desired TM_{m10} mode. Thus, a more precise circuit model is required for the discussion of stable TM_{m10}-mode operation; this circuit model also enables us to discuss TM_{0n0}-mode ($n \geq 3$) operation.

This paper deals with window-output-type combiners in the TM_{0n0} and TM_{m10} modes of operation. In Section II, we clarify analytically power-combining modes and the condition for ensuring stable desired-mode operation using the averaged potential theory [11], [12] on the basis of an appropriate equivalent circuit model for the combiner. In Section III we give the experimental results for the behavior of the TM_{0n0}-mode combiner in the case of $n = 2$, 3, and 4, and in Section IV for the TM_{m10}-mode combiner in the case of $m = 2$ and 8.

II. Mode Analysis

A. Circuit Model

Fig. 1 shows the configuration of the cylindrical cavity power combiner with an output window. N active devices are placed with uniform spacing near the periphery of the cavity of radius R. In the mode analysis of the multiple-device cavity we assume no axial field variation because of moderate cavity height and negligible power dissipation in the cavity. Dividing the radius and the periphery of the cavity into equal N_r and N_ϕ parts, respectively, we can obtain the circuit model of the multiple-device cavity shown in Fig. 2(a). Nodes denoted by A and B correspond to elements with and without device posts, respectively. Each element can be represented by the equivalent circuit shown in Fig. 2(b), where C_s is the capacitance and L_r and L_ϕ are the inductances in the radial and the azimuthal direction, respectively. The device current J_k appearing in the equivalent circuit for the element having the kth device post (Fig. 2(b)) is assumed to have a simple cubic nonlinearity, which is described by

$$J_k = -gv_k + \frac{4}{3}\theta v_k^3, \qquad 1 \leq k \leq N. \tag{1}$$

The load effect of the output window is represented by connecting the load conductance g_L at a peripheral node. All the nodes are numbered in series in both the radial and the azimuthal direction, and are designated by the coordinates (r_λ, ϕ_μ), where $\lambda = 0, 1, 2, \cdots, N_r$ and $\mu = 1, 2, \cdots, N_\phi$. The nodes with the active device and that with the load conductance are expressed by $(r_D, \phi_{D,k})$ $(k = 1, 2, \cdots, N)$ and (r_L, ϕ_L), respectively.

Manuscript received December 19, 1986; revised April 28, 1987. This work was supported in part by a Grant-in-Aid for Fundamental Research from the Ministry of Education in Japan and in part by a Research Grant from the Hōsō-Bunka (Broadcasting Culture) Foundation.

The authors are with the Department of Electronics, Okayama University, Okayama 700, Japan.

IEEE Log Number 8715979.

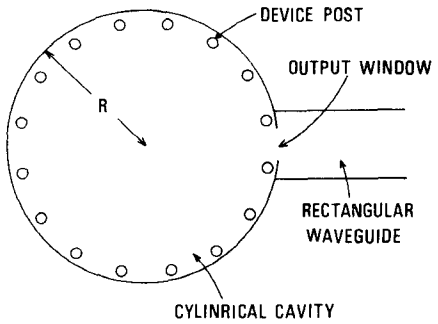

Fig. 1. Window output cylindrical cavity power combiner.

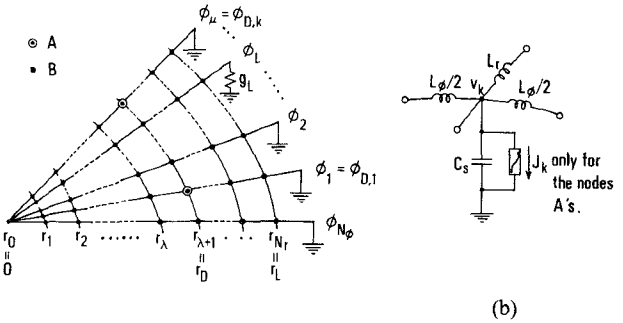

(b)

Fig. 2 Circuit model of a cylindrical cavity combiner. $C_s = c_0 r\Delta r\Delta\phi$, $L_r = l_0\Delta r/(r\Delta\phi)$, and $L_\phi = l_0 r\Delta\phi/\Delta r$ with $\Delta r = R/N_r$ and $\Delta\phi = 2\pi/N_\phi$, where c_0 is the capacitance per unit area and l_0 is the inductance per unit length and unit cross-sectional area.

Normal modes can be defined in the network without J_k's and g_L, which is called the generating system. The modes are designated by (m, n), where m $(=0,1,2,\cdots, N_\phi - 1)$ and n $(=1,2,\cdots, N_r)$ describe the number of voltage variations in the azimuthal and the radial direction, respectively. The oscillation frequency of the mode (m, n), ω_{mn}, and its voltage amplitude at the node (r_λ, ϕ_μ), $p_{mn}(r_\lambda, \phi_\mu)$,[1] become equal to the resonant frequency and the electric field distribution of the TM_{mn0} mode, respectively, in the limit $N_r \to \infty$ and $N_\phi \to \infty$. Because of the symmetry of the generating system with respect to the center, the system has twofold degenerate modes. A degenerate-mode pair, denoted as (m, n) and $(\tilde{m}, n)$, have spatial patterns which differ only in phase by $\pi/2$ along the periphery. Each node voltage can be given using the normal-mode expansion as

$$v(r_\lambda, \phi_\mu; t) = \sum_{n=1}^{N_r} \sum_{m=0}^{N_\phi - 1} A_{mn} p_{mn}(r_\lambda, \phi_\mu) \cos(\omega_{mn} t + \psi_{mn}),$$
$$0 \leqslant \lambda \leqslant N_r, \quad 1 \leqslant \mu \leqslant N_\phi. \quad (2)$$

B. Averaged Potential

The behavior of the system can be discussed using the averaged potential of the system [11], [12]. The averaged potential of the system of Fig. 2 is given by the time average of integrals of the currents through both positive and negative conductances, that is, active devices and load, as

$$U = \text{time average of} \sum_{k=1}^{N} \int J_k\, dv_k + \int g_L v_L\, dv_L \quad (3)$$

where

$$v_k = v(r_D, \phi_{D,k}), \qquad 1 \leqslant k \leqslant N$$
$$v_L = v(r_L, \phi_L).$$

Substituting (1) and (2) into (3), we obtain

$$\frac{U}{4} = -\sum_{m,n} \alpha_{mn} A_{mn}^2 + \frac{1}{2} \sum_{m,n} \sum_{m',n'} \theta_{mn,m'n'} A_{mn}^2 A_{m'n'}^2 + \frac{1}{2} \sum_{m,n} \theta_{mn,\tilde{m}n} A_{mn}^2 A_{\tilde{m}n}^2 \cos 2\Psi_{mn} + \frac{1}{8} \sum_{m,n} \sum_{m',n'} \xi_{mn,\tilde{m}n,m'n',\tilde{m}'n'} \cdot A_{mn} A_{\tilde{m}n} A_{m'n'} A_{\tilde{m}'n'} \cos\Psi_{mn} \cos\Psi_{m'n'} \quad (4)$$

where

$$\alpha_{mn} = g \sum_{k=1}^{N} p_{mn,k}^2 - g_L p_{mn,L}^2 \quad (5a)$$

$$\theta_{mn,m'n'} = \theta(2 - \delta_{mn,m'n'}) \sum_{k=1}^{N} p_{mn,k}^2 p_{m'n',k}^2 \quad (5b)$$

$$\xi_{mn,\tilde{m}n,m'n',\tilde{m}'n'} = \theta \sum_{k=1}^{N} p_{mn,k} p_{\tilde{m}n,k} p_{m'n',k} p_{\tilde{m}'n',k} \quad (5c)$$

and

$$\Psi_{mn} = \psi_{mn} - \psi_{\tilde{m}n}. \quad (6)$$

In (5), simplified notations are used, such as

$$p_{mn,k} \equiv p_{mn}(r_D, \phi_{D,k}), \qquad 1 \leqslant k \leqslant N$$
$$p_{mn,L} \equiv p_{mn}(r_L, \phi_L).$$

The summation in the third and fourth terms of the right-hand side of (4) should be made over all the degenerate-mode pairs. The quantity α_{mn} is a small-signal gain parameter of mode (m, n) and $\theta_{mn,mn}$ and $\theta_{mn,m'n'}$ $((m, n) \neq (m', n'))$ are called the self- and mutual-saturation parameters.

According to the averaged potential theory [11], [12] the stable stationary states correspond to the minimum points of U. Thus, it is noted that, from (4) and (5), the mode amplitude and the phase of steady oscillation, A_{mn} and ψ_{mn}, together with the stability condition, are given using the parameters α_{mn} and $\theta_{mn,m'n'}$, which are determined by p_{mn} values at the active devices and at the load.

C. Power-Combining Modes

Consider a steady state in which only one mode, say mode (m, n), is excited. The amplitude of steady oscilla-

[1] The voltage distribution $p_{mn}(r_\lambda, \phi_\mu)$ is normalized as

$$\sum_{r_\lambda = 0}^{N_r} \sum_{\phi_\mu = 1}^{N_\phi} p_{mn}(r_\lambda, \phi_\mu)\, p_{m'n'}(r_\lambda, \phi_\mu) = \delta_{mn,m'n'}$$

where $\delta_{mn,m'n'}$ is the Kronecker delta.

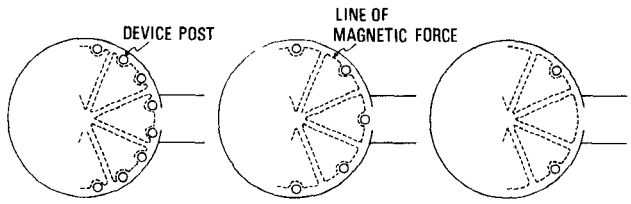

Fig. 3. TM_{m10}-mode combiner containing N devices. The dashed lines represent lines of magnetic force. (a) $N = 4m$. (b) $N = 2m$. (c) $N = m$.

tion is determined from

$$\partial U/\partial A_{mn}^2|_{A_{mn}\neq 0,\ \text{others}=0} = 0$$

as

$$A_{mn,0}^2 = \alpha_{mn}/\theta_{mn,mn}. \tag{7}$$

As the amplitude of v_L is given by $A_{mn,0}p_{mn,L}$, we have, for the output power $P_0(m,n)$,

$$P_0(m,n) = \frac{1}{2}g_L(A_{mn,0}p_{mn,L})^2 = \frac{g\sum_{k=1}^{N} p_{mn,k}^2 - g_L p_{mn,L}^2}{2\theta\sum_{k=1}^{N} p_{mn,k}^4}\cdot g_L p_{mn,L}^2. \tag{8}$$

In the case where $p_{mn,L} \neq 0$, the maximum output power for this mode is given by

$$P_{0,\max}(m,n) = \frac{g^2}{8\theta}\cdot\frac{\left(\sum_{k=1}^{N} p_{mn,k}^2\right)^2}{\sum_{k=1}^{N} p_{mn,k}^4} \tag{9}$$

for the corresponding optimum load conductance $g_{L,\text{opt}}(m,n)$ such as

$$g_{L,\text{opt}}(m,n) = \frac{g}{2}\cdot\frac{1}{p_{mn,L}^2}\sum_{k=1}^{N} p_{mn,k}^2. \tag{10}$$

Equation (9) shows that $P_{0,\max}(m,n)$ reaches the maximum value $N_g^2/(8\theta)$ for the modes in which the voltage amplitudes at the device sites $|p_{mn,k}|, 1 \leqslant k \leqslant N$, are equal to one another. Accordingly, perfect power combining is basically possible in such a mode, because the available power of an active device having the current–voltage characteristic of (1) is given by $g^2/(8\theta)$ [13]. Typical power combiners which satisfy the above condition are as follows: the TM_{0n0} $(n \geqslant 1)$-mode combiner having an arbitrary number of devices, N, and the TM_{m10}-mode combiner $(m \geqslant 1)$ containing N devices, where $N = 4m - \nu$, $2m - \nu$, and $m - \nu$, with $\nu = 0,1,2\cdots$. Some of the TM_{m10}-mode combiners are depicted in Fig. 3.

D. Stability Condition

The stability condition can be derived from the criterion of the averaged potential minimum. First, for the stability of a single mode, say mode (m,n), the necessary and sufficient condition is given by

$$\left.\frac{\partial U}{\partial A_{m'n'}^2}\right|_{A_{mn}=A_{mn,0},\ \text{all others}=0} = -\alpha_{m'n'} + \Theta_{m'n',mn}A_{mn,0}^2 > 0 \quad \text{for all } (m',n') \neq (m,n) \tag{11}$$

where

$$\Theta_{m'n',mn} \equiv \left(1 - \frac{\delta_{m'n',\tilde{m}n}}{2}\right)\theta_{m'n',mn}. \tag{12}$$

Next, in order for l $(\geqslant 2)$ modes (m_1,n_1), (m_2,n_2), $\ldots,(m_l,n_l)$ to form a stable simultaneous multimode oscillation, the necessary condition is obtained as

$$\left|\frac{\partial U}{\partial A_{m'n'}^2}\right|_{\substack{A_{m_in_i}=A_{m_in_i,s}(i=1,2,\cdots,l)\\ \text{all others}=0}} = -\alpha_{m'n'} + \sum_{i=1}^{l}\Theta_{m'n',m_in_i}A_{m_in_i,s}^2 > 0 \quad \text{for all } (m',n') \neq (m_i,n_i),\quad i=1,2,\cdots,l \tag{13}$$

where $A_{m_in_i,s}(i=1,2,\cdots,l)$ is the steady-state amplitude of mode (m_i,n_i) given by

$$A_{m_in_i,s}^2 = \frac{\begin{vmatrix} \Theta_{m_1n_1,m_1n_1} & \Theta_{m_1n_1,m_2n_2} & \cdots & \alpha_{m_1n_1} & \cdots & \Theta_{m_1n_1,m_ln_l} \\ \Theta_{m_2n_2,m_1n_1} & \Theta_{m_2n_2,m_2n_2} & \cdots & \alpha_{m_2n_2} & \cdots & \vdots \\ \vdots & & & \vdots & & \vdots \\ \Theta_{m_ln_l,m_1n_1} & \cdots & \cdots & \alpha_{m_ln_l} & \cdots & \Theta_{m_ln_l,m_ln_l} \end{vmatrix}}{\begin{vmatrix} \Theta_{m_1n_1,m_1n_1} & \Theta_{m_1n_1,m_2n_2} & \cdots & \Theta_{m_1n_1,m_ln_l} \\ \Theta_{m_2n_2,m_1n_1} & \Theta_{m_2n_2,m_2n_2} & \cdots & \vdots \\ \vdots & & \ddots & \vdots \\ \Theta_{m_ln_l,m_1n_1} & \cdots & \cdots & \Theta_{m_ln_l,m_ln_l} \end{vmatrix}} \quad i=1,2,\cdots,l. \tag{14}$$

(only the ith column)

Both (11) and (13) have the physical meaning that the corresponding steady-state oscillation makes the growth of any other modes impossible.

E. Undesired-Mode Suppression

To obtain stable power-combining operation, we must make the desired power-combining mode, say mode (m_0, n_0), the only mode to be excited in the system with the load conductance $g_{L,\mathrm{opt}}(m_0, n_0)$. This can be brought about by suppressing all the undesired modes. In order to absorb undesired modes without any effect on the desired mode, we introduce conductances $g_s(r_\lambda, \phi_\mu)$ between the earth and the nodes at which $p_{m_0,n_0}(r_\lambda, \phi_\mu) = 0$. The modification of the averaged potential due to $g_s(r_\lambda, \phi_\mu)$ can be represented by reducing the small-signal gain parameter α_{mn} in (5a) by $\Delta\alpha_{mn}$, where

$$\Delta\alpha_{mn} = \sum_{r_\lambda, \phi_\mu} g_s(r_\lambda, \phi_\mu) p_{mn}^2(r_\lambda, \phi_\mu). \tag{15}$$

Note that $\Delta\alpha_{mn}$ is zero for the desired mode (m_0, n_0). For both the undesired single mode (m_1, n_1) and the undesired multiple modes (m_1, n_1), $(m_2, n_2), \cdots, (m_l, n_l)$ to be unstable to permit the growth of the desired mode, the following condition must be satisfied:

$$\alpha_{m_0 n_0} - \sum_{i=1}^{l} \theta_{m_0 n_0, m_i n_i} A_{m_i n_i, s}^2 > 0 \tag{16}$$

where $l = 1$ and $A_{m,n,s} = A_{m_1 n_1, 0}$ only for the single-mode case. Inequality (16) is obtained by putting $(m', n') = (m_0, n_0)$ and reversing the inequality sign in (11) and (13). Use of appropriate values of $g_s(r_\lambda, \phi_\mu)$'s enables $A_{m_i n_i, s}$, which decreases as shown in (7) and (14), to satisfy (16).

III. TM_{0n0}-Mode Power Combining

A. Structure of the Multiple-Device Cavity

Power combining experiments were carried out for the cylindrical TM_{0n0}-mode combiners for the cases where $n = 2$, 3, and 4 using GD511A Gunn diodes, manufactured by the Nippon Electric Company. The radius of each combining cavity, R, was determined in order for the oscillation frequency to be nearly equal to 9.2 GHz. The configuration of the TM_{040}-mode combiner, for example, is shown in Fig. 4, where d, s, and h are, respectively, the diameter of the device post, the spacing between the device post and the cavity wall, and the cavity height. The structural dimensions of each combiner used in the experiments are shown in Table I. The output window of width d_w together with the stub tuner of depth d_s at distance l_s from the window is used for adjusting the load admittance.

The working frequency range of the diodes was approximately from 7.4 GHz to 11.4 GHz by measurements using a conventional waveguide Gunn oscillator structure. Table II shows the resonant frequencies of relevant normal modes of the TM_{040}-mode combiner cavity with an effective radius of 61.0 mm. The number of undesired modes whose frequencies are within the working range of active devices increases rapidly with the order number of the power-combining mode, n.

The conductances $g_s(r_\lambda, \phi_\mu)$ for the suppression of undesired modes in our cylindrical cavity were realized using microwave absorber rings of conductance G_a, width h_a,

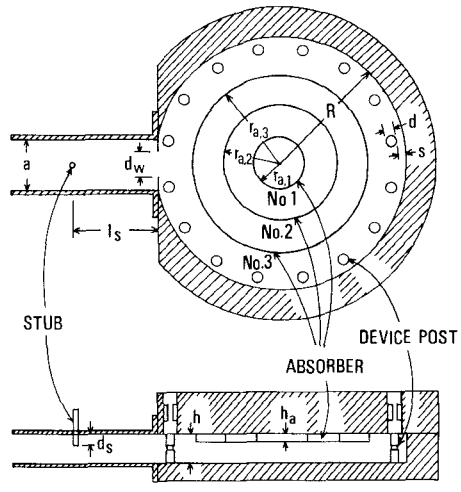

Fig. 4. Configuration of the TM_{040}-mode combiner ($a = 22.9$ mm).

TABLE I
STRUCTURAL DIMENSIONS OF TM_{0n0}-MODE COMBINERS

Power-combining mode	Number of diodes, N	R (mm)	d (mm)	s (mm)	h (mm)
TM_{020}	8	30.0	3.0	1.0	10.2
TM_{020}	15	32.0	3.0	2.0	10.2
TM_{030}	16	46.8	3.0	1.0	10.2
TM_{040}	16	62.5	3.0	1.0	10.2

TABLE II
RESONANT FREQUENCIES (IN GHZ) OF NORMAL MODES IN THE TM_{040}-MODE COMBINER CAVITY
Effective cavity radius = 61.0 mm.

m	TM_{m10}	TM_{m20}	TM_{m30}	TM_{m40}
0				9.22
1			7.96	10.42
2			9.09	11.57
3		7.63	10.18	
4		8.65	11.24	
5		9.65		
6	7.77	10.63		
7	8.67	12.54		
8	9.56			
9	10.44			
10	11.32			

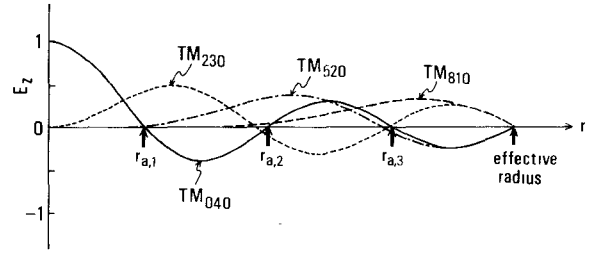

Fig. 5. Profiles of radial distribution of electric field (E_z) for the desired modes and some typical undesired modes in a TM_{040}-mode combiner.

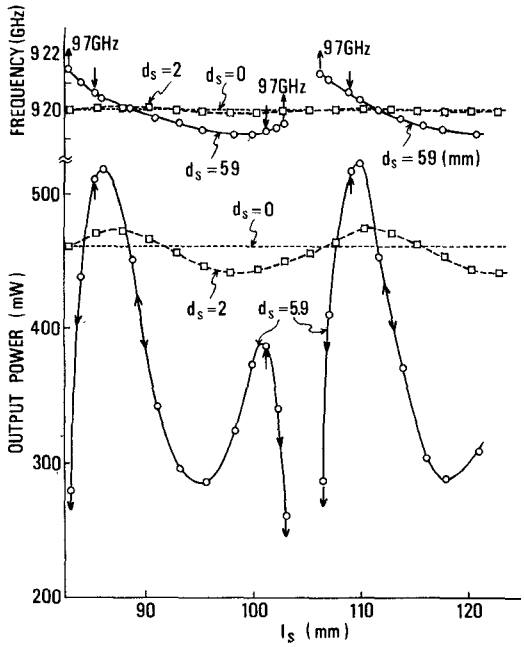

Fig. 6. Behavior of the TM_{040}-mode combiner for variation of the stub depth d_s and position l_s in the case where $d_w = 11.0$ mm. The following microwave absorbers were used[3]: absorber no. 1, $G_a = 0.23$ m℧, $h_a = 3$ mm; absorber nos. 2 and 3, $G_a = 0.059$ m℧, $h_a = 2$ mm.

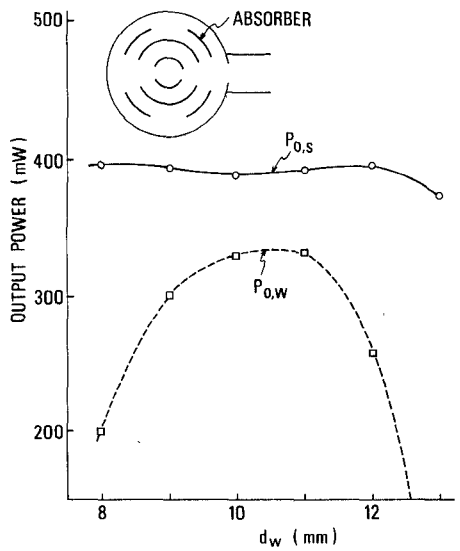

Fig. 7. Output power of the TM_{040}-mode combiner with the absorbers of $G_a = 1.4$ m℧ and $h_a = 3$ mm.[3] $P_{0,w}$ denotes the output power for $d_s = 0$, and $P_{0,s}$ the maximum output power obtained by stub adjustment.

and thickness 0.15 mm placed at the position of vanishing electric field for the desired TM_{0n0} mode, as shown in Fig. 4. Fig. 5 gives, as an example, the profiles of electric field distribution for the desired mode and some typical undesired modes in the TM_{040}-mode power combiner cavity. It will be obvious that the small-signal gain parameters of all undesired modes can effectively be reduced by placing microwave absorbers along all the circles of vanishing electric field for the desired mode.

B. Power-Combining Operation

In the case where no absorbers are introduced into the combiner cavities for $n = 2$, 3, and 4, desired-mode oscillation can be excited only for appropriate load conductance; it is inevitably replaced by an undesired mode without reaching the maximum output power. These experimental results confirm that suppression of undesired modes is indispensable for stable power-combining operation.

Fig. 6 shows a typical experimental result which illustrates the behavior of the TM_{040}-mode combiner with such absorbers for the variation of the stub depth d_s and position l_s in the case where $d_w = 11.0$ mm. For small d_s, the desired-mode oscillation follows the application of bias voltage and is sustained for the variation of l_s. For a certain large value of d_s, when l_s is varied, mode jump takes place from the desired mode into a certain undesired mode after passing the output power maximum, and the reverse mode jump occurs before reaching the output power maximum.

The range of l_s in which only the desired mode is stable can be increased by use of a sufficiently strong absorber, but this is at the expense of a reduction in power-combining efficiency. Fig. 7 shows the output power $P_{0,w}$ of the TM_{040}-mode combiner for the case where $d_s = 0$ and the maximum output power obtained by stub adjustment, $P_{0,s}$, for several values of d_w under stronger absorption than in Fig. 6.[2] In the case where $d_s = 0$, $P_{0,w}$ increases with d_w as long as d_w is below a certain value; this was the same tendency as in TM_{020}- and TM_{030}- mode power combining. The value of $P_{0,s}$ is almost independent of d_w as long as d_w is not so small. The difference between $P_{0,s}$ and the maximum value of $P_{0,w}$ was almost zero in TM_{020}-mode combining, but was not small in TM_{030}- and TM_{040}-mode combining. However, it is considered that the difference can be reduced to almost zero by adjusting the position of the output window, as seen in the experimental result of TM_{810}-mode combining (see Section IV-B).

TABLE III
MAXIMUM POWER-COMBINING EFFICIENCY IN THE TM_{0n0}-MODE COMBINER

Power-combining mode \ Number of diodes, N	8	16
TM_{020}	100% (9.22GHz)	83% (9.20GHz)*
TM_{030}	—	76 (9.19GHz)
TM_{040}	—	73 (9.20GHz)

Oscillation frequency given in parentheses.
*Result for the 15-diode combiner.

The maximum power-combining efficiency in the TM_{0n0}-mode combiner is shown in Table III. The efficiency is defined here as the ratio of the maximum output power of the combiner, in which desired mode operation is ensured

[2] In the experiment shown in Figs. 6 and 7, broken-type absorbers were used (see the top of Fig. 7). This was effective for improving the combining efficiency.

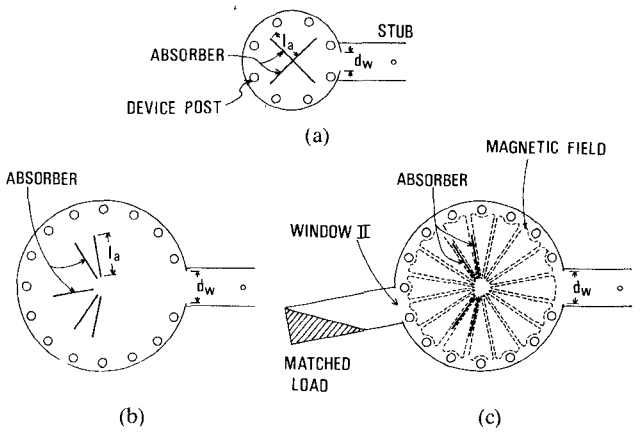

Fig 8. TM_{m10}-mode combiners used in the experiments. (a) TM_{210}-mode combiner. (b) TM_{810}-mode combiner (structure no. 1). (c) TM_{810}-mode combiner (structure no. 2).

by use of adequate absorbers, to the sum of output powers of each diode properly measured using an ordinary waveguide oscillator structure at the same frequency. In TM_{020}-mode combining, perfect power combining was achieved in the octuple-diode case ($N = 8$), although combining efficiency decreased by doubling the number of diodes. In the case where $N \cong 16$, the combining efficiency decreased with larger n for TM_{0n0}-mode combining. It is considered that this decrease in combining efficiency is due to the decrease of coupling between the diodes and the electromagnetic field in the cavity [14].

The external Q factors, Q_{ex}'s, of the TM_{0n0}-mode combiners listed in Table III were measured by the method of injection locking. Typical results are as follows: $Q_{ex} = 127$ for the TM_{020}-mode combiner of $N = 8$, and $Q_{ex} = 758$ for the TM_{040}-mode combiner of $N = 16$.

IV. TM_{m10}-Mode Power Combining

A. Structure of the TM_{m10}-Mode Power Combiners

Experiments of TM_{m10}-mode power combining were performed for the case where $m = 2$ and $m = 8$ using the multiple-device cavities shown in Fig. 8. For TM_{210}-mode power combining of eight ($= 4m$) devices, the same structural dimensions as for the TM_{020}-mode combiner with eight devices were used (see Table I). Similarly, the same dimensions as for TM_{040}-mode combining were employed for TM_{810}-mode combining, although the number of active devices was reduced to 15 ($= 2m - 1$) so as to permit adequate magnetic coupling of the cavity mode with the waveguide mode.

As is shown in (a) and (b) of Fig. 8, microwave absorbers were laid out in a radial manner in order to ensure proper coupling of the desired cavity mode with the waveguide mode[3] and to suppress all the relevant undesired cavity modes. In TM_{810}-mode combining, another combiner structure, shown in Fig. 8(c), was tried, where an auxiliary window (window II) was prepared and connected with a matched load. Note that this matched load gives, in principle, no power dissipation to the desired TM_{810} mode because of the magnetic field distribution shown in Fig. 8(c).

B. Power-Combining Operation

The behavior of the TM_{210}-mode and TM_{810}-mode combiners for the variation of stub depth d_s and position l_s is similar to that of the TM_{0n0}-mode combiners shown in Fig. 6.

An experimental comparison between the two types of TM_{810}-mode combiners, shown in (b) and (c) of Fig. 8, gave the result that the maximum combining efficiency was higher in the latter type than in the former by about 5 percent. It is probable that the symmetry of the electromagnetic field in the cavity can be improved to some degree by the presence of window II; such an improvement can decrease power dissipation in the absorbers[4] and increase the total sum of output powers generated by each diode to give higher combining efficiency. It was confirmed experimentally that the power loss due to window II was less than 1.5 percent of the output power.

The output powers of the TM_{210}-mode combiner and the TM_{810}-mode one shown in Fig. 8(c), $P_{0,\omega}$ and $P_{0,s}$, defined in Section III-B, for several values of the window width d_w are plotted in Fig. 9. The maximum power-combining efficiencies are given in Table IV. In the TM_{210}-mode combiner, almost perfect power combining can be achieved merely by adjusting the width of the output window, as in the TM_{020}-mode combiner with the same number of diodes. In the TM_{810}-mode combiner, $P_{0,s}$ tends to increase gradually with d_w. The maximum value of $P_{0,s}$ was considerably larger than that of $P_{0,w}$, as in the TM_{030}- and the TM_{040}-mode combiner. This maximum efficiency could also be obtained without a stub tuner by shifting the window of $d_w \cong 11.0$ mm from the aperture of the cavity to an appropriate position in the output waveguide. Tables III and IV indicate that the combining efficiency is better in the TM_{810}-mode combiner than in the TM_{040}-mode one, although both combiner cavities have the same structural dimensions. This is considered to be due to stronger coupling between the diodes and the electromagnetic field in the former, since electromagnetic energy is distributed more intensively near the periphery of the cavity in the TM_{810} mode than in the TM_{040} mode.

Measured Q_{ex} values of the TM_{210}- and the TM_{810}-mode combiner listed in Table IV were 233 and 1620, respectively.

[3] In the case where no absorbers are introduced, the stable oscillation in the TM_{m10} mode takes the pattern configuration which is obtained by rotating the mode pattern of Fig 8(a) by $\pi/4$ for $m = 2$ and gives no output power; this can be derived from the principle of the averaged potential minimum.

[4] In TM_{m10}-mode power combining with large m, a decrease in symmetry of the electromagnetic field causes considerable power dissipation due to the absorbers because of large spatial variation of the electric field in the azimuthal direction.

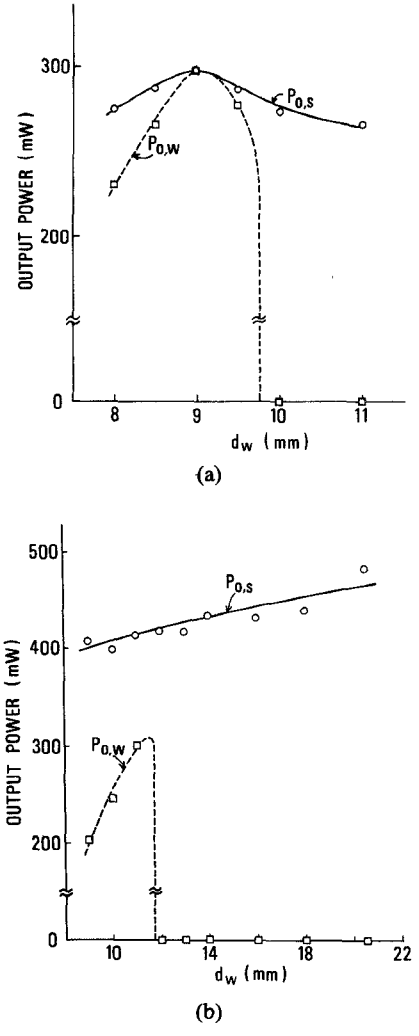

Fig. 9. Output power of the TM_{m10}-mode combiners. (a) TM_{210}-mode combiner, with $G_a = 0.22$ m℧, $h_a = 2$ mm, and $l_a = 20$ mm. (b) TM_{810}-mode combiner, with $G_a = 0.23$ m℧, $h_a = 3$ mm, and $l_a = 25$ mm.

TABLE IV
MAXIMUM POWER-COMBINING EFFICIENCY IN THE TM_{m10}-MODE COMBINER

Power-combining mode \ Number of diodes, N	8	15
TM_{210}	98% (8.59GHz)	—
TM_{810}	—	88% (9.70GHz)

V. CONCLUSIONS

For cylindrical-cavity multiple-device structures of the window-output type, we have analyzed the power-combining capability of the TM_{0n0} and the TM_{m10} ($m \geq 1$) mode and the condition for suppression of undesired modes. The analytical results have been confirmed by experiments for TM_{0n0}-mode combiners of $n = 2$, 3, and 4 and TM_{m10}-mode combiners of $m = 2$ and 8.

The experimental results obtained are summarized as follows.

(1) Almost perfect power combining in the TM_{210} mode can be achieved using an octuple-diode structure, as in the TM_{020} mode, and the combining efficiency decreases with increasing n or m.
(2) The combining efficiency is considerably higher in the TM_{810}-mode combiner than in the TM_{040}-mode one when multiple-diode structures with the same structural dimensions are used.

These results are seen as suggesting that, for higher mode combining, the combining efficiency strongly depends on the coupling of the diodes to the electromagnetic field in the combiner cavity and that TM_{m10}-mode combining is preferable for the oversized-cavity combiner to TM_{0n0}-mode combining. A detailed investigation of the device–field coupling in various power-combining modes is highly desired.

In TM_{m10}-mode combiners with large m, it seems that the use of an appropriate auxiliary window (described in Section IV-A) can bring, in addition to undesired-mode suppression, improvement in the symmetry of the electromagnetic field in the cavity to give higher combining efficiency; the quantitative estimation remains for future work.

The use of the TM_{m10}-mode combiner as an amplifier is another interesting subject to be investigated, whereby sufficient device–field coupling, as referred to above, is considered to be essential also for obtaining broad bandwidth.

ACKNOWLEDGMENT

The authors wish to thank N. Ueda, S. Ono, and T. Kishimoto for their considerable assistance in the course of experiments.

REFERENCES

[1] K. J. Russell, "Microwave power combining techniques," *IEEE Trans. Microwave Theory Tech.*, vol. MTT-27, pp. 472–478, May 1979.
[2] K. Chang and C. Sun, "Millimeter-wave power-combining techniques," *IEEE Trans. Microwave Theory Tech.*, vol. MTT-31, pp. 91–107, Feb. 1983.
[3] R. S. Harp and H. L. Stover, "Power combining of *X*-band IMPATT circuit modules," in *1973 IEEE-ISSCC Dig.*, Feb. 1973, pp. 118–119.
[4] R. Aston, "Techniques for increasing the bandwidth of a TM_{010}-mode power combiner," *IEEE Trans. Microwave Theory Tech.*, vol. MTT-27, pp. 479–482, May 1979.
[5] M. Dydyk, "Efficient power combining," *IEEE Trans. Microwave Theory Tech.*, vol. MTT-28, pp. 755–762, July 1980.
[6] C. A. Drubin, A. L. Hieber, G. Jerinic, and A. S. Marinilli, "A 1 kW_{peak}, 300 W_{avg} IMPATT diode injection locked oscillator," in *1982 IEEE MTT-S Symp. Dig.*, May 1982, pp. 126–128.
[7] K. Fukui, S. Nogi, and T. Sato, "Stable power-combining mode operation of a cylindrical cavity multiple-device oscillator" (in Japanese), *Trans. Inst. Electron. Commun. Eng. Japan*, vol. J68-B, pp. 1011–1019, Sept. 1985.
[8] R. G. Mastroianni and A. C. Levitan, "High power stable pulsed *X*-band IMPATT amplifiers using resonant cavity power combiners," in *1978 IEEE MTT-S Symp. Dig.*, June 1978, pp. 1–6.
[9] K. Fukui and S. Nogi, "Mode analytical study of cylindrical cavity power combiners," *IEEE Trans. Microwave Theory Tech.*, vol. MTT-34, pp. 943–951, Sept. 1986.

[10] S. Nogi and K. Fukui, "Power-combining operation of window-output cylindrical cavity multiple-device structures" (in Japanese), *Trans. Inst. Electron. Commun. Eng. Japan*, vol. J69-C, pp. 964–973, Aug. 1986.
[11] M. Kuramitsu and F. Takase, "An analytical method for multimode oscillators using the averaged potential," (in Japanese), *Trans. Inst. Electron. Commun. Eng. Japan*, vol. J66-A, pp. 336–343, Apr. 1983.
[12] M. Kuramitsu and F. Takase, "The analysis of the square array of van der Pol oscillators using the averaged potential," *Int. J. Nonlinear Mechanics*, vol. 20, pp. 395–406, May 1985.
[13] K. Fukui and S. Nogi, "Power combining ladder network with many active devices," *IEEE Trans. Microwave Theory Tech.*, vol. MTT-28, pp. 1059–1067, Oct. 1980.
[14] S. Nogi, Y. Sadakane, and K. Fukui, "On the coupling between electromagnetic field and device-posts in multiple-device cylindrical cavities," (in Japanese), *IECE Japan*, Tech. Rep. MW86-10, May 1986.

Shigeji Nogi was born in Osaka Prefecture, Japan, on December 26, 1945. He received the B.E., M.E. and D.Eng. degrees in electronics engineering from Kyoto University, Kyoto, Japan, in 1968, 1970, and 1984, respectively.

From 1970 to 1972, he was employed by the Central Research Laboratory, Mitsubishi Electric Corporation, Amagasaki, Japan. In 1972 he joined the Department of Electronics, Okayama University, where he has been engaged in research on microwave active circuits, multimode oscillators, and nonlinear wave propagation.

Dr. Nogi is a member of the Institute of Electronics and Communication Engineers of Japan.

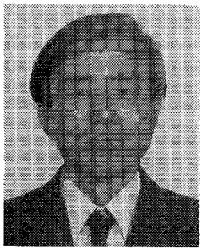

Kiyoshi Fukui (M'75) was born in Tokushima Prefecture, Japan, on January 13, 1930. He received the B.Sc. degree in physics in 1952 and the D.Eng. degree in electronics engineering in 1964, both from Kyoto University, Kyoto, Japan.

From 1958 to 1962, he was a Research Assistant in the Department of Electronics, Kyoto University. From 1962 to 1967, he taught as an Assistant Professor at the Training Institute for Engineering Teachers, Kyoto University. In 1967, he became a Professor of Electronics at the Himeji Institute of Technology, Himeji, Japan. Since 1971, he has been with the Department of Electronics, Okayama University. During the 1977–78 academic year, he was a Visiting Professor at the University of Wisconsin at Madison. His research interests have been mainly in such nonlinear phenomena in electronics as locking phenomena in oscillators, frequency multiplication by variable capacitance, behavior of multiple-device structures, and nonlinear wave propagation.

Dr. Fukui is a member of the Institute of Electronics and Communication Engineers of Japan and the Physical Society of Japan.